Evidence for Native-Defect Donors in *n*-Type ZnO

D. C. Look,[1,2] G. C. Farlow,[1] Pakpoom Reunchan,[3] Sukit Limpijumnong,[3,4] S. B. Zhang,[4] and K. Nordlund[5]

[1]*Semiconductor Research Center, Wright State University, Dayton, Ohio 45435, USA*

[2]*Materials and Manufacturing Directorate, Air Force Research Laboratory, Wright-Patterson Air Force Base, Ohio 45433, USA*

[3]*School of Physics, Suranaree University of Technology and National Synchrotron Research Center, Nakhon Ratchasima, Thailand*

[4]*National Renewal Energy Laboratory, Golden, Colorado 80401, USA*

[5]*Accelerator Laboratory, University of Helsinki, FIN-00014, Helsinki, Finland*

(Received 5 August 2005; published 21 November 2005)

Recent theory has found that native defects such as the O vacancy V_O and Zn interstitial Zn_I have high formation energies in *n*-type ZnO and, thus, are not important donors, especially in comparison to impurities such as H. In contrast, we use both theory and experiment to show that, under N ambient, the complex Zn_I-N_O is a stronger candidate than H or any other known impurity for a 30 meV donor commonly found in bulk ZnO grown from the vapor phase. Since the Zn vacancy is also the dominant acceptor in such material, we must conclude that native defects are important donors and acceptors in ZnO.

DOI: 10.1103/PhysRevLett.95.225502 PACS numbers: 61.72.Ji, 71.55.Gs, 72.20.Fr, 78.55.Et

Semiconducting ZnO has generated great interest in the past decade because of advances in bulk and epitaxial growth that have opened the door for new photonic and electronic applications, such as UV light emitting diodes and transparent transistors [1,2]. Previous research had established that ZnO was always *n*-type and that the dominant donors were usually shallow with activation energies of between 30 and 60 meV [3,4]. Because it was also known that the crystal growth was typically Zn-rich, the dominant donor was almost always identified as either the O vacancy V_O or the Zn interstitial Zn_I [5,6]. This model was strongly challenged in the year 2000 when Kohan *et al.* showed theoretically that both V_O and Zn_I have high formation energies in *n*-type ZnO and that, furthermore, both are deep, not shallow, donors [7]. More recent theory has concluded that Zn_I is actually a shallow donor, rather than deep [8,9], as has also been suggested by electron-irradiation experiments [6]; however, its high formation energy would still limit its participation in the conductivity of *n*-type material. Also in the year 2000, the defect-donor model was further challenged by Van de Walle's theoretical result that H is always a donor in ZnO, that it is easily ionized, and that it has a low enough formation energy to be abundant; thus, Van de Walle suggested that it was likely to be a dominant background donor in ZnO materials that were exposed to H during growth [10]. This proposal has been amenable to testing, because H-containing, high-quality, bulk ZnO, grown by a seeded chemical vapor transport (SCVT) technology, has been commercially available for the past few years. For the most part, these tests have confirmed that a shallow donor due to H exists in SCVT ZnO and can contribute significantly to the conductivity [11–16]. This fact, coupled with the theoretical evidence of high formation energies for the native donors [7], has led to a prevailing opinion that native donors do not play a significant role in the conductivity of as-grown ZnO. In contrast, we will offer evidence here that native donors can contribute significantly to conduction in ZnO but as complexes, rather than isolated elements.

The main sample used in this study was a 5 mm × 5 mm × 0.42 mm piece cut from a wafer grown by the SCVT technique at ZN Technology, Inc. [17]. Material of this type is of very high quality, with peak electron mobility >2000 $cm^2/V\,s$, 300 K carrier concentration in the 10^{16} cm^{-3} range, and photoluminescence (PL) linewidths under 0.5 meV, as shown in Figs. 1 and 2 [4]. The sample was first annealed at 715 °C, in order to release most of the H [14,15], then was irradiated with high-energy electrons to create point defects, and finally was annealed again at temperatures from 200–500 °C, in order to investigate the annihilation of the point defects. As seen in Fig. 1, several sharp PL lines appear in the region 3.357–3.365 eV, and these spectral features are usually assigned to transitions of excitons bound to neutral donors (D^0X transitions), in which the donor remains in its ground state ($n = 1$) during the transition. Some of these lines have been tentatively identified; for example, the lines at 3.35964 eV (I_8 or I_{8a} in

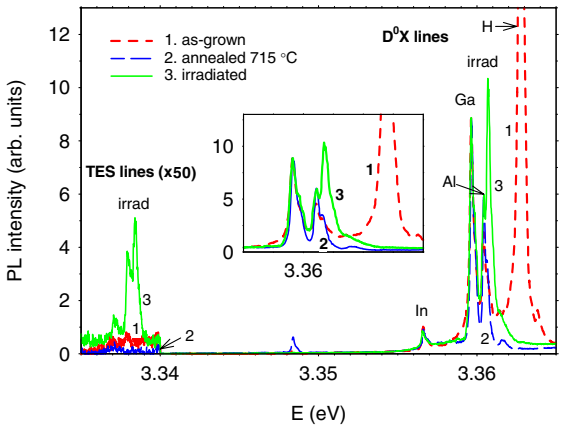

FIG. 1 (color online). 4-K photoluminescence spectra for ZnO sample. The inset shows the D^0X lines in greater detail.

the literature) and 3.36042 eV (I_6 or I_{6a}) have been assigned to Ga_{Zn} and Al_{Gn}, respectively. (See Ref. [18] for an excellent review of PL in ZnO.) All of the spectra presented in this work are normalized to the I_8 line, because it is relatively isolated and also not expected to change significantly as a result of annealing or irradiation treatments. However, the most dominant PL line in this particular sample before annealing is the D^0X line at 3.36270 eV (I_4), now almost universally assigned to interstitial H [16,18]. This identification results at least partially from annealing experiments, because I_4 disappears for anneals above 600 °C, in good correlation with the effusion of H from the sample [14–16,19]. Our sample behaves in the same way, as evidenced by the strong reduction of I_4 after an anneal of 715 °C (curve 2 in Fig. 1). Not shown in Fig. 1 is a two-electron satellite (TES) replica of I_4, appearing at 3.32961 eV. A TES transition is one in which the donor is left in an excited $n = 2$ state after the collapse of the exciton. If the donor associated with I_4 follows a hydrogenic model, then the ground-state ($n = 1$) energy of this donor should be given by $4/3(3.36270 - 3.32961) = 44.1$ meV. Other TES transitions, also not shown, are seen near 3.32 eV and may be associated with I_6 and I_8 [18]. If so, then the hydrogenic model would predict ground-state energies of 53–55 meV for these donors, presumably associated with Ga_{Zn} and Al_{Zn}. Thus, the donors identified from PL are H, at 44 meV, and Ga_{Zn} and Al_{Zn}, at about 55 meV.

To create point defects, we have used the Van de Graaff electron accelerator at Wright State University. The sample was irradiated on the Zn face (0001) with 1 MeV electrons three separate times, making a total fluence of 3×10^{17} cm^{-2}. The PL spectrum after the third irradiation is presented as curve 3 in Fig. 1. A new sharp defect line at 3.36070 eV, which we will designate as I_D, is generated by the irradiation. Concomitantly, a triplet feature, comprised of energies 3.33711, 3.33793, and 3.33840 eV, is also generated. These we will designate $I_{D,\mathrm{TES1}}$, $I_{D,\mathrm{TES2}}$, and $I_{D,\mathrm{TES3}}$. This triplet has an intensity about 100 times less than that of I_D, and this reduction is about the same as that observed for the TES line of H compared with its parent line, I_4. Thus, the defect triplet at 3.338 eV clearly is related to I_D, and, if the hydrogenic model holds, the associated energy is $4/3(3.3607 - 3.3379) \approx 30.4$ meV. This value is less than that predicted from an empirical version of Haynes' rule presented in Ref. [18]. However, that version was developed for simple, isolated impurities, Al, Ga, In, and H, and there is no reason to expect that it should hold for a defect-related complex. Both I_D and its TES triplet are greatly reduced for anneals greater than 500 °C (not shown), evidently due to defect recombination. It is important to note at this point that the as-grown sample, represented by curve 1 in Fig. 1, has two small lines at the energies of $I_{D,\mathrm{TES1}}$ and $I_{D,\mathrm{TES2}}$, respectively, and possibly also a line in the I_D region, although obscured by I_6. This is our first indication that the *as-grown* sample contains defect-related donors.

We next discuss the temperature-dependent mobility μ and carrier concentration n, shown in Fig. 2. To avoid clutter, we show curves representing only four stages in the evolution of this sample: (1) as-grown; (2) annealed at 715 °C for 1/2 hour in flowing N_2 gas; (3) irradiated with 1 MeV electrons, in three equal stages up to a total fluence of 3×10^{17} cm^{-2}; and (4) annealed at 400 °C, following previous anneals beginning at 200 °C. It should be noted that a final anneal at 500 °C (not shown) eliminated almost all of the irradiation damage and basically returned the μ and n curves to those of stage 2. [Note that a return to the μ and n curves of stage 1 (as-grown) is of course impossible, because the H content was lost in stage 2, the first 715 °C anneal.]

The mobility data (inset in Fig. 2) were fitted to an accurate charge-carrier scattering theory, described elsewhere [20], and the only fitting parameter was the acceptor concentration N_A. The carrier concentration data of Fig. 2 were then fitted to the charge-balance equation:

$$n + N_A = \sum_i \frac{N_{Di}}{1 + n/\phi_{Di}}, \tag{1}$$

where the subscript i denotes a particular donor and where ϕ_{Di} is a function of T and E_{Di}, the donor energy [cf. Eq. (8) of Ref. [20]]. The fitting parameters in Eq. (1) are the donor concentrations (N_{Di}'s), donor energies (E_{Di}'s), and acceptor concentration N_A. Excellent fits to the n vs $1/T$ data in Fig. 2 were obtained by also including a degenerate surface layer in the analysis [20,21].

The PL results discussed above determined the energies of three different donors, calculated from their respective TES lines: 55 meV, possibly associated with Ga_{Zn} and/or Al_{Zn}; 44 meV, associated with H; and 30 meV, produced by irradiation and thus associated with a defect. Indeed, the 30 and 44 meV energies turn out to be good fitting parameters for two of the three donors required to fit our Hall-effect data, but the third donor is best fitted with about 75 meV, rather than 55 meV. The carrier concentration fits are

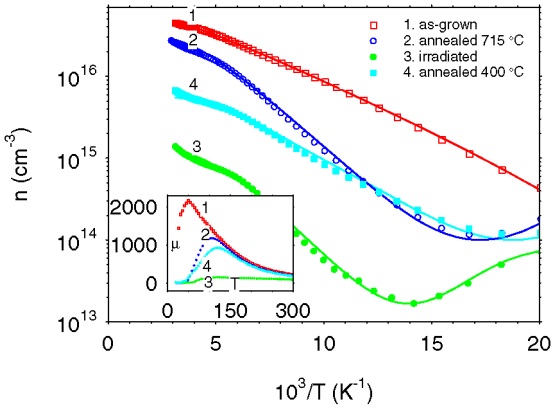

FIG. 2 (color online). Temperature-dependent carrier concentration for ZnO sample. The solid lines are theoretical fits. The inset shows the experimental mobility curves after the same four treatments.

shown as solid lines in Fig. 2, and the fitting parameters are given in Table I. Two major conclusions are evident from the results: (1) the 44 meV H level essentially disappears during the 715 °C anneal, in agreement with the PL data; and (2) a 30 meV level is produced by irradiation but also exists in the as-grown sample and the sample annealed at 715 °C. It should be emphasized that the choice of 30 meV as a Hall fitting parameter is not dependent on the fact that the PL analysis also found a donor at 30 meV. Indeed, a donor of this energy has been found previously by a number of groups to give good fits to ZnO Hall-effect data [3,4,6]. To help identify this 30 meV donor, we appeal to theory.

First of all, we calculate the expected 1 MeV-electron-bombardment production rates of Zn and O Frenkel pairs from molecular dynamics simulations [22]. The threshold energies were calculated by giving a randomly chosen O or Zn atom a recoil energy in a random direction in an experimentally controlled angular window of 15 degrees around the desired (0001) direction. The interatomic interaction model for the ZnO system will be published elsewhere [23], but the potential development principles are described in Ref. [24]. To account for the experimental situation with a beam acceptance angle, the threshold was determined as the average over the direction-specific thresholds obtained within the 15° angular window.

For Zn-face (0001) irradiation at 300 K, the threshold for O displacement is 44 eV, and that for Zn displacement, 34 eV. We then apply the McKinley-Feshbach relativistic cross-section formula [25] to give effective production rates of 0.18 cm^{-1} for O displacement and 0.30 cm^{-1} for Zn displacement. Thus, we would expect that our fluence of 3×10^{17} cm^{-2} would produce O_I and V_O concentrations of about 5×10^{16} cm^{-3} and Zn_I and V_{Zn} concentrations of about 9×10^{16} cm^{-3}. Either of these numbers is consistent with the observed 30 meV donor concentration of about 2×10^{17} cm^{-3} in the irradiated sample (see Table I), because the value 2×10^{17} cm^{-3} is actually an upper limit. That is, the mobility after such a heavy irradiation is almost certainly reduced by electrical inhomogeneity, and, thus, it is artificially low, leading to artificially high donor and acceptor concentrations. However, the concentration of Zn_I should still be about twice that of V_O, and, moreover, there is abundant evidence that V_O is a deep, not shallow, donor [7–9,26]. Thus, Zn_I is a much better candidate for the irradiation donor than V_O. However, there also is evidence that isolated Zn_I is mobile at room temperature, so that it likely has to form a complex to be stable [27,28].

A search for potential complexing partners for Zn_I immediately suggests N, which easily substitutes for O in the ZnO lattice and which indeed has a concentration of about 10^{17} cm^{-3} in ZnO material of the type we are using [29]. Thus, we have examined the formation energy, binding energy, and $(0/+)$ transition energy of the complex Zn_I-N_O using first principles calculations. We applied density functional theory (DFT) within the local density approximation (LDA) and used Vanderbilt-type ultrasoft pseudopotentials, as implemented in the VASP code [30]. To obtain defect formation energies, defined elsewhere [31,32], a supercell approach was used, with a ZnO supercell size of 96 atoms. The main result of the calculation is that the binding energy of the Zn_I-N_O complex is about 0.9 eV; thus, the complex should be stable at room temperature. The formation energies of the N_O, Zn_I, and Zn_I-N_O species in ZnO depend on the Fermi energy and the partial pressures of the elements or, in other words, the chemical potentials of the elements, during growth. The secondary-ion mass-spectroscopy measurements [29] found a N concentration [N] of about 1×10^{17} cm^{-3}. Based on our calculated formation energies of N_O, Zn_I, and Zn_I-N_O, together with the measured N concentration ($[N] = [N_O] + [Zn_I\text{-}N_O]$), we estimate a N chemical potential of 0.92 eV below the N_2 precipitation limit (assuming Zn-rich and charge-neutral growth conditions and a growth temperature of 950 °C). The calculated formation energy [33] shows that, during growth, N_O^- acts as the dominant acceptor and Zn_I^{2+} as the dominant donor, with the Fermi energy pinned at about 1.0 eV above the valence band where the two defects have approximately the same energy, about 1.4 eV. The corresponding defect concentrations are on the order of 10^{17} cm^{-3}. The concentration of the Zn_I-N_O complex is about 2 orders of magnitude lower, as determined from the reaction $N_O + Zn_I \rightarrow Zn_I\text{-}N_O + 0.9$ eV and the associated detailed-balance relationship $[N_O][Zn_I]/N_{site}[Zn_I\text{-}N_O] = \exp(-E_b/kT)$. Here we use $N_{site}(ZnO) = 4.28 \times 10^{22}$ cm^{-3} and $E_b = 0.9$ eV. At $T = 950$ °C, we get $[Zn_I\text{-}N_O]/[Zn_I] = 0.012$, which means that only about 1/100 of the Zn_I ions take part in formation of the complex. However, during cool-down, it is expected that the formation of the complex will accelerate, assuming a sufficiently low Zn_I diffusion barrier. As the temperature cools to about 500 °C, the quantity $[Zn_I\text{-}N_O]/[Zn_I]$ approaches unity, which means that about half of the Zn_I are already bound in the com-

TABLE I. Fitting parameters for mobility and carrier concentration data.

	E_{D1} (meV)	N_{D1} (10^{16} cm^{-3})	E_{D2} (meV)	N_{D2} ($10^{16}cm^{-3}$)	E_{D3} (meV)	N_{D3} ($10^{16}cm^{-3}$)	N_A ($10^{16}cm^{-3}$)
As-grown	30	0.45	44	3.0	75	2.0	0.13
715 °C	30	0.74			75	3.2	0.7
Irradiated	30	~20			75	0.13	~20
400 °C	30	1.35			75	0.4	1.2

plexes. At room temperature, $[Zn_I\text{-}N_O]/[Zn_I] \approx 10^9$, so that nearly 100% of the Zn_I are in complexes. With other impurities (such as H_I) in the sample, the above balance conditions would vary somewhat, but the main conclusions should remain the same.

The electronic transition energy of Zn_I-N_O is somewhat uncertain, due to the well-known LDA gap error. However, our calculations show that the donor level of Zn_I-N_O is shallower than that of isolated Zn_I, which itself is argued to be a shallow donor [8,9]. In addition, a wave function analysis of Zn_I shows delocalization, which is characteristic of a shallow level. In short, although the $(0/+)$ transition energy of Zn_I-N_O cannot be accurately calculated, it is entirely consistent with the observed value of 30 meV. Further details of these calculations will be published elsewhere.

It is also interesting to compare the 0.9 eV binding energy with the activation energy for irradiation-defect annealing in ZnO, measured previously as 1.7 eV [34]. The difference between these two energies, 0.8 eV, should be the motional energy for Zn_I and is a reasonable value for an interstitial.

Other evidence for a Zn_I-N_O complex comes from optically detected magnetic resonance experiments in epitaxial N-doped ZnO [35]. An observed spin-1/2 center was consistent with a Zn interstitial, possibly in association with an N atom, since it was not observed in a sample with lower N content. Besides Zn_I, other donors, such as H, are also believed to associate with N [14,36]. However, H-N would be neutral, whereas Zn_I-N has a shallow-donor level.

Finally, other Zn_I-acceptor complexes that behave as shallow donors are also predicted to be stable. For example, very recently Wardle *et al.* [37] have used DFT to show that Zn_I-Li_{Zn} is bound by 0.7 eV and has a shallow-donor transition. This result further strengthens and generalizes our assertion that Zn_I-related shallow donors can exist and be important in as-grown ZnO.

In summary, we have carried out extensive low-temperature photoluminescence and temperature-dependent Hall-effect measurements on irradiated ZnO and have identified a defect-related donor at about 30 meV, which also exists in as-grown ZnO. We have further carried out molecular dynamics simulations, to show that the expected production rate of Zn_I is consistent with the concentrations of the 30 meV donor after irradiation, and density functional calculations to show that the Zn_I-N_O defect complex is a shallow donor with a sufficient binding energy to explain the annealing data. Thus, the conclusion is that native-defect-related donors can exist in *n*-type ZnO and contribute to its conductance.

D. C. L. and G. C. F. were supported by U.S. Air Force (F33615-00-C-5402), ARO (W911NF05C0024), SVTA, Inc., and Structured Materials Industries, Inc. (41471-010605-01). P. R. and S. L. were supported by AFOSR/AOARD (FA5209-05-P-0309) and TRF (BRG4880015 and PHD/0203/2546). Work at NREL was supported by DOE/BES and EERE (DE-AC36-99GO10337).

[1] D. C. Look, Mater. Sci. Eng. B **80**, 383 (2001).
[2] S. J. Pearton *et al.*, Prog. Mater. Sci. **50**, 293 (2005).
[3] P. Wagner and R. Helbig, J. Phys. Chem. Solids **35**, 327 (1974).
[4] D. C. Look *et al.*, Solid State Commun. **105**, 399 (1998).
[5] F. A. Kröger, *The Chemistry of Imperfect Crystals* (North-Holland, Amsterdam, 1964).
[6] D. C. Look, J. W. Hemsky, and J. R. Sizelove, Phys. Rev. Lett. **82**, 2552 (1999).
[7] A. F. Kohan *et al.*, Phys. Rev. B **61**, 15 019 (2000).
[8] F. Oba *et al.*, J. Appl. Phys. **90**, 824 (2001).
[9] S. B. Zhang, S.-H. Wei, and A. Zunger, Phys. Rev. B **63**, 075205 (2001).
[10] C. G. Van de Walle, Phys. Rev. Lett. **85**, 1012 (2000).
[11] S. F. J. Cox *et al.*, Phys. Rev. Lett. **86**, 2601 (2001).
[12] D. M. Hofmann *et al.*, Phys. Rev. Lett. **88**, 045504 (2002).
[13] K. Shimomura, K. Nishiyama, and R. Kadono, Phys. Rev. Lett. **89**, 255505 (2002).
[14] N. H. Nickel and K. Fleischer, Phys. Rev. Lett. **90**, 197402 (2003).
[15] K. Ip *et al.*, Appl. Phys. Lett. **82**, 385 (2003).
[16] Y. M. Strzhemechny *et al.*, Appl. Phys. Lett. **84**, 2545 (2004).
[17] ZN Technology, 910 Columbia Street, Brea, CA 92821, USA.
[18] B. K. Meyer *et al.*, Phys. Status Solidi B **241**, 231 (2004).
[19] D. C. Look *et al.*, Phys. Status Solidi A **195**, 171 (2003).
[20] D. C. Look, Semicond. Sci. Technol. **20**, S55 (2005).
[21] D. C. Look and R. J. Molnar, Appl. Phys. Lett. **70**, 3377 (1997).
[22] J. Nord, K. Nordlund, and J. Keinonen, Phys. Rev. B **68**, 184104 (2003).
[23] P. Erhart, K. Albe, N. Juslin, and K. Nordlund (to be published).
[24] J. Nord *et al.*, J. Phys. Condens. Matter **15**, 5649 (2003).
[25] F. Agullo-Lopez, C. R. A. Catlow, and P. D. Townsend, *Point Defects in Materials* (Academic, New York, 1988).
[26] P. Kasai, Phys. Rev. **130**, 989 (1963).
[27] Yu. V. Gorelkinskii and G. D. Watkins, Phys. Rev. B **69**, 115212 (2004).
[28] C. Coşkun *et al.*, Semicond. Sci. Technol. **19**, 752 (2004).
[29] D. C. Look *et al.*, Appl. Phys. Lett. **81**, 1830 (2002).
[30] G. Kresse and J. Furthmüller, Comput. Mater. Sci. **6**, 15 (1996).
[31] S. B. Zhang and J. E. Northrup, Phys. Rev. Lett. **67**, 2339 (1991).
[32] S. Limpijumnong *et al.*, Phys. Rev. Lett. **92**, 155504 (2004).
[33] See EPAPS Document No. E-PRLTAO-030548 for the calculated defect formation energy. This document can be reached via a direct link in the online article's HTML reference section or via the EPAPS homepage (http://www.aip.org/pubservs/epaps.html).
[34] D. C. Look *et al.*, Appl. Phys. Lett. **75**, 811 (1999).
[35] G. N. Aliev *et al.*, Phys. Rev. B **70**, 115206 (2004).
[36] N. Ohashi *et al.*, J. Appl. Phys. **93**, 6386 (2003).
[37] M. G. Wardle, J. P. Goss, and P. R. Briddon, Phys. Rev. B **71**, 155205 (2005).